Article

Biomass to H2: Evaluation of the Impact of PV and TES Power Supply on the Performance of an Integrated Bio-Thermo-Chemical Upgrading Process for Wet Residual Biomass

Matteo Baldelli [ID], Lorenzo Bartolucci *[ID], Stefano Cordiner, Giorgio D'Andrea, Emanuele De Maina * and Vincenzo Mulone

Department of Industrial Engineering, University of Rome "Tor Vergata", Via del Politecnico,1, 00133 Rome, Italy; matteo.baldelli@uniroma2.it (M.B.); cordiner@uniroma2.it (S.C.); giorgio.dandrea.en@alumni.uniroma2.eu (G.D.); mulone@uniroma2.it (V.M.)
* Correspondence: lorenzo.bartolucci@uniroma2.it (L.B.); emanuele.de.maina@uniroma2.it (E.D.M.)

Abstract: The last Intergovernmental Panel on Climate Change (IPPC) assessment report highlighted how actions to reduce CO_2 emissions have not been effective so far to achieve the 1.5 C limit and that radical measures are required. Solutions such as the upgrading of waste biomass, the power-to-X paradigm, and an innovative energy carrier such as hydrogen can make an effective contribution to the transition toward a low-carbon energy system. In this context, the aim of this study is to improve the hydrogen production process from wet residual biomass by examining the advantages of an innovative integration of anaerobic digestion with thermochemical transformation processes. Furthermore, this solution is integrated into a hybrid power supply composed of an electric grid and a photovoltaic plant (PV), supported by a thermal energy storage (TES) system. Both the performance of the plant and its input energy demand—splitting the power request between the photovoltaic system and the national grid—are carefully assessed by a Simulink/Simscape model. The preliminary evaluation shows that the plant has good performance in terms of hydrogen yields, reaching 5.37% $kg_{H2}/kg_{biomass}$, which is significantly higher than the typical value of a single process (approximately 3%). This finding demonstrates a good synergy between the biological and thermochemical biomass valorization routes. Moreover, thermal energy storage significantly improves the conversion plant's independence, almost halving the energy demand from the grid.

Keywords: hydrogen; waste biomass; energy transition; integrated biomass conversion

1. Introduction

The sixth assessment report of the Intergovernmental Panel on Climate Change (IPPC) highlights the need to take action to mitigate climate change. In the report, global greenhouse gas emissions have not reached their peak yet, and reaching the temperature increase limit of +1.5 °C is expected to occur with a high degree of confidence. This confirms how the actions adopted so far to reduce CO_2 emissions have not been effective, and radical measures are required to keep the temperature as low as possible [1,2].

In this perspective, novel concepts are emerging in the energy field. First, bioenergy is increasingly relevant for the sustainable production of bio-based fuels and energy carriers [3–6]. Several paths can be followed to convert raw biomass into valuable products, and the choice of the best option strongly depends on its physical and chemical characteristics. However, the integration of more stages of valorization can improve the energy conversion of feedstock [4–6]. Furthermore, since biomass carbon dioxide emissions can be considered neutral along their life cycle [7–9], bioenergy, combined with carbon capture and storage (BECCS), is a potential way to significantly reduce the emissions, potentially achieving an overall carbon negative process [7–9].

Another main issue for the energy transition is the production of power from non-programmable renewable energy sources. The installed capacity of these conversion plants is required to increase considerably, according to the energy transition pathway [10], and this growing penetration requires the definition of strategies to manage the demand-production mismatch [11–13]. Electrochemical batteries are a potential solution for local and daily energy storage, but other solutions are required for a longer storage period [14,15]. From this perspective, the power-to-X paradigm has been recognized as an effective strategy. Indeed, it allows storing energy for long periods by means of the production of stable energy carriers, and it also allows the linking of different energy sectors.

Among the energy carriers, hydrogen is one of the most interesting due to its potential for decarbonization. Its main advantages are as follows: (i) The absence of carbon dioxide emissions during its use. (ii) The flexibility to be used in different applications such as light- and heavy-duty transport [16], rail mobility, heat and electricity production, and possible use in other sectors such as the chemical industry for the production of fertilizers or polymers [17] and other hard to abate processes.

In the last few years, the topic of bio-based energy carrier production has been investigated in several studies. In particular, the integration of different processes to maximize the exploration of energy potential from input biomasses emerges as a trend from the literature analysis. Trieb et al. [18] explored the production of liquid fuel by an integrated conversion process for the upgrading of waste biomass, powered both by non-programmable renewable energy and electricity provided by an internal combustion engine fueled with biogas, reaching a conversion efficiency of 53%. Poluzzi et al. [19] analyzed the recent studies on biomass upgrading via gasification-based pathways, evaluating the results through power-to-X and power-to-H_2 concepts, highlighting the need for more detailed analysis. The Technical University of Denmark, in collaboration with Aalborg University, proposed different studies [3,20–22] where the flexible operation of a biomass energy was upgraded into a methanol plant. They developed both a 75 kW two-stage reactor and an integrated numerical model for the simulation of the overall plant, which can produce both methanol (in case of local renewable energy surplus) and electricity (in case of peak demand from the grid), according to a flexible transition from one operation to the other. They found a maximum overall efficiency of 70.5% achieved by including a complete methanol production process, while the efficiency in the case of electricity production is limited to 37%. Moreover, the main challenge highlighted in the study consists of the capability to operate the solid oxide fuel cell (SOFC) using cleaned pyrolysis gas. In fact, several issues arise due to tars and hydrocarbons affecting the SOFC's durability. The integration of pyrolysis and sorption-enhanced gasification has been analyzed in [23], where the goal of the plant is the production of both hydrogen and drop-in biofuels from softwood. In this work, an Aspen Plus model is used to investigate the impact of some process parameters, such as pyrolysis temperature, Steam/Biochar, and Sorbent/Biochar. These results showed how the pyrolysis temperature affects the product distribution while the other parameters affect the energy conversion efficiency. Moreover, the article highlights that process integration leads to improved mass conversion yield and increases overall energy efficiency by up to 10%.

Regarding wet biomasses, anaerobic digestion (AD) is a widely diffused process for their energy conversion. However, it has some limitations in converting waste biomass since microorganisms have poor degradation efficiency with specific biomass components [24]. For this reason, some studies have analyzed the integration of the incomplete exploitation of biomass energy potential. In [25], the integration of AD and gasification has been evaluated with the goal of maximizing the overall efficiency of the process to produce gaseous fuel (biogas from AD and syngas from gasification). In [26], a life cycle analysis of the co-gasification of sewage sludge, coming from an anaerobic digestion system, and woody biomass has been performed, showing how the synergy of the system can increase the energy recovery up to 24% compared to the separate process. In [27], a comparison between double-stage AD and single-stage AD coupled with the pyrolysis of digestate has

been performed. Their results show how the coupling of AD with pyrolysis increases the energy yield to 6.1 MJ/kg$_{VS}$ (kg of volatile substance), while the double-step digestion only yields 2.6 MJ/kg$_{VS}$.

The literature review has shown a lack in the study of the enhancement of hydrogen production from the AD by its coupling with other processes and still requires further insights. From this perspective, the aim of this paper is then to explore an innovative integrated bio-thermochemical route to produce a high purity hydrogen stream from wet residual biomass and, in particular, to analyze the mass and energy yields and the theoretical energy outputs and efficiencies. Moreover, in order to evaluate the plant's performance in an energy transition scenario, a hybrid power supply is considered. The plant is powered by a photovoltaic system (PV), a thermal energy storage (TES) system, and the electric grid. Particular emphasis is given to the evaluation of the power demand of the plant and the power source split to understand the advantages and impacts of their integration in the plant supply mix, with the aim of limiting the energy withdrawn by the grid.

In order to obtain high purity hydrogen, innovative biomass by-product upgrading processes, such as electrified steam reforming and a membrane reactor, are included in the plant. A Simulink/Simscape model is developed for the preliminary evaluation of the overall process performance characteristics in terms of hydrogen production, global energy and conversion efficiency, and CO_2 emission comparison between the different scenarios.

The paper is structured as follows: Firstly, information about the methodology considered is provided, along with a description of the plant, feedstock characteristics, and assumptions. In the results section, three different case studies about the plant operation are described, and the main findings are reported. Finally, in the discussion section, a comparison between the three cases is carried out, highlighting the major contributions of the study.

2. Materials and Methods

2.1. Plant Description

The plant aims at producing hydrogen while maximizing the exploitation of available residual biomasses by integrating several thermochemical processes, such as anaerobic digestion (AD), pyrolysis (Py), oil reforming (P-Ref), and syngas reforming (Ref). The performance parameters of the proposed plant were evaluated through a numerical model developed in the MatLab/Simulink/Simscape environments.

As shown in Figure 1, the biomass enters first in the AD, where it produces a biogas composed mainly of carbon dioxide and methane. After a hydraulic retention time of 41 days, the remaining solid part is transferred to a dryer and then to a pyrolizer, where a fast pyrolysis at 500 °C occurs. The three products of pyrolysis follow different routes. The solid part (char) goes into a burner, where its chemical energy is converted into heat to supply the energy needed for drying the digestate and maintaining the pyrolysis process. The liquid part (bio-oil) is composed of two main parts: an organic fraction, which can be suitable for the production of bio-based fuels, and an aqueous fraction. The gaseous part (pyro-syngas) goes into a reformer, together with the other gaseous streams coming from AD and P-Ref, where a hydrogen-enriched syngas and a CO_2-enriched purge gas are obtained. Finally, a Pd-catalytic membrane separates high purity hydrogen from the remaining part of the syngas.

From an energy point of view, the system is powered by the chemical energy of the residual biomass and external electricity. Electric power is obtained from a PV plant, which is supported by the grid to ensure the continuous operation of the plant. The electricity powers up the compressor upstream of the catalytic membrane, and it can also be converted to supply thermal energy to the anaerobic digester, pyrolizer, and the two reformers.

To increase the energy independence of the plant from the grid, a TES is included. The role of the TES is to maximize the exploitation of the PV, converting the electricity surplus into heat that can be later used to supply the thermal energy demand of the plant.
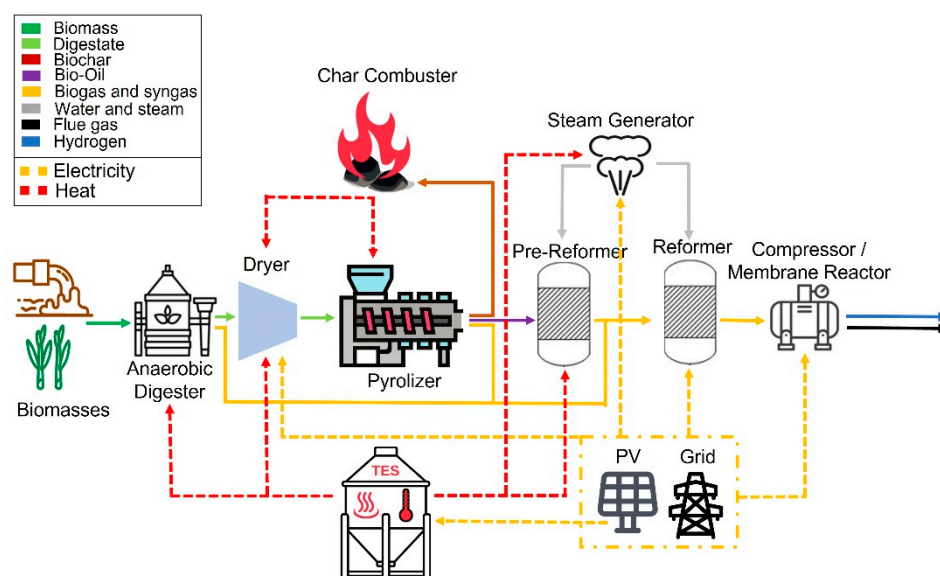
Figure 1. Plant mass and energy flows.

Details of the component models are reported in the Appendix A. The pyrolysis [28,29] and PV models have been validated in comparison with experimental data in previous works [30]. The AD and membrane reactor performance parameters have been assumed from the literature studies, while the reforming model developed in MatLab is validated in this work, as reported in the results section.

Three different scenarios are compared in this work. In Scenario 1, the whole plant is powered only by the grid. This scenario is taken as a reference condition for comparison with the plant powered by renewable energy. In Scenario 2, the plant demand is supplied not only by the grid but also by a photovoltaic system. Finally, in Scenario 3, a TES supports the system's operation by supplying heat energy stored from the surplus of the PV system. Moreover, waste heat recovery is also explored. There are three different sources: the cooling of hydrogen-rich syngas before the condensation of the membrane reactor, the bio-oil latent heat [31], and the cooling process of the flow at the outlet of the membrane reactor. These heat fluxes are used in the plant for the steam generator's pre-heating. Furthermore, the demand for energy from the pyrolysis reactor is self-produced by burning the biochar, which has a low heating value of approximately 28 MJ/kg, according to [31].

The system design is based on the pyrolysis reactor. In fact, the pyrolysis model used in this paper was developed and validated for a lab-scale shaftless screw reactor presented by the authors in previous works [28,29]. The model is designed for an inlet mass flow of 1 kg/h, which is the constraint used to size the other components of the plant. The PV maximum power is set to satisfy twice the plant's design maximum load to ensure good operation stability. The main parameters describing the design are reported in Table 1, while a more detailed description of the model is presented in the Appendix A.

Table 1. Main design parameters of the plant. The geometrical and operating parameters of the pre-reformer and reformer are taken from the reference [32].

Anaerobic Digester		Pyrolizer		PV System	
Temperature [°C]	35 ± 2	length [m]	0.25	Panel power (W)	285
Specific Methane Production $\left[\mathrm{Nl_{CH_4}} \middle/ \mathrm{kg_{vs}} \right]$	237	diameter [m]	0.02	Numbers of panels	63
Hydraulic Retention Time [Days]	41	Screw rotational speed [rpm]	45	System power (kW)	18
Organic Load Rate $\left[\mathrm{kg_{vs}} \middle/ \mathrm{m^3 \cdot day} \right]$	2	temperature [°C]	500		

Table 1. *Cont.*

Pre-reformer		Reformer		TES	
Length [m]	0.7	Length [m]	0.7	Capacity [kWh]	700
Diameter [mm]	12.7	Diameter [mm]	12.7	Initial capacity [kWh]	300
Temperature [°C]	378.05	Temperature [°C]	866	T max [°C]	1200
Steam/Carbon	1	Steam/Carbon	2	Heat loss in 24 h	<2%

2.2. Feedstock

According to the EU Directive 2018/2001 [33] and recent scientific literature, only residual biomasses were investigated in this study. The advantages of the use of residual biomass are several: (i) no competition with the food and feed sectors; (ii) no additional emissions for their production; and (iii) the possibility to avoid post-treatment for their disposal.

In the proposed plant, a combination of two residual biomasses is taken as input: quinoa residues and wastewater sludge. The types of biomass and the operating conditions of the process are taken from the study proposed by Tayibi et al. [6]. Data on specific methane production, organic load, proximate analysis, and detailed analysis of the digestate are reported in Table 2. The feedstock mixture of quinoa residues and wastewater sludge is divided in terms of volatile matter fraction, with 45% for quinoa and 55% for wastewater sludge, respectively.

Table 2. Elemental and proximate analysis, polymeric composition, and low heating value of the biomasses. The proximate analysis provides the weight percentages (%wt) of the dry matter (DM) and volatile substances (VS). The characterization of the biomasses is taken from Ref. [6] to allow a direct comparison of the results of the present study.

Parameters	Quinoa Residues	Wastewater Sludge
DM (%$_{wt}$)	90.1 ± 0.1	18.7 ± 0.1
VS (%$_{wt,DM}$)	88.9 ± 0.3	79.6 ± 2.2
C (%$_{wt}$)	43.3 ± 0.2	41.2 ± 0.2
H (%$_{wt}$)	6.0 ± 0.1	6.2 ± 0.2
N (%$_{wt}$)	0.2 ± 0.0	7.0 ± 0.2
S (%$_{wt}$)	0.1 ± 0.0	0.6 ± 0.0
O (%$_{wt}$)	40.5 ± 0.3	41.2 ± 0.5
Cellulose (%$_{wt}$)	24.6 ± 0.4	-
Hemicellulose (%$_{wt}$)	14.1 ± 0.5	-
Lignin (%$_{wt}$)	7.0 ± 0.3	-
Ash (%$_{wt}$)	10.0 ± 0.2	3.8 ± 0.4
Mass flow (kg/year)	2972	19,550
Low Heating Value (MJ/kg)	14.05	-

2.3. Power Demand

The power demand is evaluated for each subsystem. It depends mainly on the working temperature and weather conditions, as reported in Table 3. The power demand of the components is calculated as the output of the numerical model (described in the Appendix A) or taken from the literature.

2.4. KPIs of the Plant

In this section, the key performance indicators (KPIs) used to evaluate the performance of the plant are described. A literature analysis was made to support the selection and make the results easily comparable with other studies such as the work reported in Prestipino et al. [4], Gadsbøll et al. [21], and Bach et al. [5].

Table 3. Power demand of the system components. The drying power is derived from [34], while the power of the other components is directly evaluated from the simulation.

Component	Power [W]
Pre-reformer	1700
Reformer	3000
Steam generation	1020
Compressor	364
Pyrolizer	263
Drying	3120
AD	Depending on weather conditions (temperature)
Storage	Depending on weather conditions (PV production)

2.4.1. Hydrogen Yield

The main goal of the plant is the production of hydrogen. This makes the hydrogen yield an important parameter for evaluating the performance of the plant [4]. It can be easily calculated by integrating over the operating period the mass flow of the hydrogen ($\dot{m}_{H_2}$) and of the biomass dry matter of ($\dot{m}_{bio,dry}$) (Equation (1)):

$$Y_{H_2,mass} = \frac{\int \dot{m}_{H_2} \, dt}{\int \dot{m}_{bio,dry} \, dt} \; . \tag{1}$$

2.4.2. CO_2 Emissions

The plant's design and operation aim at achieving a minimum carbon footprint. From this perspective, it is crucial to evaluate the net CO_2 emissions of the system. The positive contribution is related to the carbon footprint of the electrical energy withdrawn from the grid, while the negative contribution is the CO_2 produced by biomass conversion and captured, and integrated over the whole operating period. In particular, the CO_2 considered is the carbon dioxide flow, which is separated through the membrane after the reformer and captured. In this work, the energy consumption and related CO_2 emissions of the transportation and storage of the captured carbon dioxide are not considered. However, the potential carbon negativity of the downstream process is accounted for in order to give a perspective on the potential of the process. The CO_2 emitted due to the combustion of char is instead considered neutral, and therefore it is not accounted for in the equation. The footprint of the system is evaluated in Equation (2). In the present calculations, the specific CO_2 emission by the grid was taken to be equal to 213.4 $\frac{g_{CO_2}}{kWh}$, according to the current Italian energy mix [35]. For the emission related to the life cycle assessment (LCA) of the PV system, a specific CO_2 emission of 48 $\frac{g_{CO_2}}{kWh}$ is considered according to [36].

$$m_{CO_2,tot} = e_{CO_2,grid} \cdot En_{grid} + e_{CO_2,PV} \cdot En_{PV,tot} - \int \dot{m}_{CO_2,fluegas} dt \, , \tag{2}$$

where:

- $e_{CO_2,grid}$ is the specific CO_2 emission of the electricity in the grid;
- En_{grid} is the yearly electricity withdrawn from the central grid;
- $e_{CO_2,PV}$ is the specific CO_2 emission of the electricity of the PV;
- $En_{PV,tot}$ is the yearly electricity production from the PV;
- $\dot{m}_{CO_2,fluegas}$ is the carbon dioxide mass flow in the flue gas after reforming.

2.4.3. Plant Efficiency

The overall efficiency of the plant (Equation (3)) is calculated as a direct measure of the biomass conversion effectiveness [4,21]. As can be observed in Equation (3), both the energy from the grid and the chemical energy of the residual biomasses are taken as inputs.

The energy output of the system consists of the chemical energy of the hydrogen produced, the organic fraction of the bio-oil, as well as the residual energy surplus stored in the TES.

The LHV_{H_2} is assumed to be equal to 33.3 $\left[\dfrac{\text{kWh}}{\text{kg}_{H_2}}\right]$ [37].

The LHV_{Oil} is assumed to be equal to 6.3 $\left[\dfrac{\text{kWh}}{\text{kg}_{Oil}}\right]$ [38].

$$\eta = \frac{m_{H_2} \cdot LHV_{H_2} + E_{stored\,,TES} + m_{oil} \cdot LHV_{oil}}{E_{ee} + m_{quinoa} \cdot LHV_{quinoa}} \tag{3}$$

where:

- m_{H_2} is the yearly hydrogen mass production;
- LHV_{H_2} is the low heating value of hydrogen;
- $E_{stored\,,TES}$ is the difference between the final and initial energy content in TES;
- m_{oil} is the yearly oil organic fraction mass production;
- LHV_{oil} is the low heating value of the organic fraction of the oil;
- E_{ee} is the energy produced by PV or absorbed from the grid;
- m_{quinoa} is the yearly quinoa mass feed (only quinoa is accounted for since the sludge does not have a proper heating value);
- LHV_{quinoa} is the low heating value of quinoa.

2.4.4. Total Specific Energy Consumption (TEC) for H2 Production

Another key parameter is the energy consumption for hydrogen production. The total energy contribution is considered, accounting also for the thermal energy content of the biomass. This value can be calculated in terms of the mass (Equation (4)) and volume (Equation (5)) of the hydrogen produced.

$$TEC_{mass} = \frac{m_{quinoa} \cdot LHV_{quinoa} + E_{ee}}{m_{H_2,tot}} \tag{4}$$

$$TEC_{vol} = \frac{m_{quinoa} \cdot LHV_{quinoa} + E_{ee}}{Vol_{H_2,tot}} \tag{5}$$

where:

- E_{ee} is the energy produced by PV or absorbed from the grid;
- m_{quinoa} is the yearly quinoa mass feed (only quinoa is accounted for since the sludge does not have a proper heating value);
- LHV_{quiona} is the low heating value of biomass;
- m_{H_2} is the yearly hydrogen mass production;
- $Vol_{H_2,tot}$ is the yearly hydrogen normal volume production.

2.4.5. Electrical Specific Energy Consumption (EEC) for H2 Production

Another interesting KPI is the specific energy consumption, which accounts only for electrical energy. Indeed, electrical energy is the only primary energy input in the system since the chosen feedstock is a mixture of residual biomasses. This parameter allows the comparison of the system's performance with that of other hydrogen production technologies, such as the electrolyzer. Moreover, this value can be calculated both in terms of mass (Equation (6)) and volume (Equation (7)) of the hydrogen produced as follows:

$$EEC_{mass} = \frac{E_{ee}}{\int \dot{m}_{H_2}\,dt}, \tag{6}$$

$$EEC_{vol} = \frac{E_{ee}}{\int \dot{Vol}_{H_2}\,dt}. \tag{7}$$

2.4.6. Specific CO_2 Emissions

To generalize the results of the system, the specific value of the emission is calculated per unit mass of hydrogen produced. The values of the overall parameter evaluated in Equation (3) are divided by the total hydrogen production, as reported in Equations (8) and (9) [4], as follows:

$$e_{CO_2,mass} = \frac{e_{CO_2,grid} \cdot En_{grid} + e_{CO_2,PV} \cdot En_{PV,tot} - \int m_{CO_2,fluegas} dt}{\int \dot{m}_{H_2} \, dt} , \tag{8}$$

$$e_{CO_2,Vol} = \frac{e_{CO_2,grid} \cdot En_{grid} + e_{CO_2,PV} \cdot En_{PV,tot} - \int m_{CO_2,fluegas} dt}{\int \dot{Vol}_{H_2} \, dt} . \tag{9}$$

where:

- $e_{CO_2,grid}$ is the specific CO_2 emission in the electricity of the grid;
- En_{grid} is the yearly electricity withdrawn from the central grid;
- $\dot{m}_{CO_2,fluegas}$ is the carbon dioxide mass flow in the flue gas;
- $e_{CO_2,PV}$ is the specific CO_2 emission of the electricity of the PV;
- $En_{PV,tot}$ is the yearly electricity production from the PV;
- m_{H_2} is the yearly hydrogen mass production;
- $Vol_{H_2,tot}$ is the yearly hydrogen normal volume production.

2.4.7. Self-Consumption (SC)

As one of the most significant differences between the three scenarios is the contribution of renewable energy sources (RES), the system self-consumption (Equation (10)) is measured. This parameter can give an idea of the effectiveness of the exploitation of renewable energy.

$$SC = \frac{En_{PV} + En_{TES}}{En_{tot}} \tag{10}$$

where:

- En_{PV} is the yearly photovoltaic electricity directly utilized by the system;
- En_{TES} is the yearly energy of TES utilized by the system;
- En_{tot} is the yearly energy consumption of the system.

3. Results and Discussion

3.1. Validation of the Reforming Model

Bio-oil is composed of several hydrocarbon compounds; however, only a few species are usually considered in the literature, such as acetic acid, ethylene glycol, and acetone [39]. The reforming section has been implemented according to the model proposed by Vagia et al. [39] and tested at a temperature ranging from 400 to 1300 K with a steam-to-carbon ratio (S/C) of six for validation against the results shown in [39].

In Figures 2–4, the results of the validation analysis are reported. To prevent carbon deposition in the catalyst, usually the pre-reformer stage works with a steam-to-carbon ratio of at least two. Although the maximum deviation from the reference is 28%, if we consider the working temperature of the pre-reformer, the maximum deviation does not exceed 5%, as shown in Figures 2–4. This is within the limits of the present analysis and has been considered good agreement between the behavior of the model and the reference.
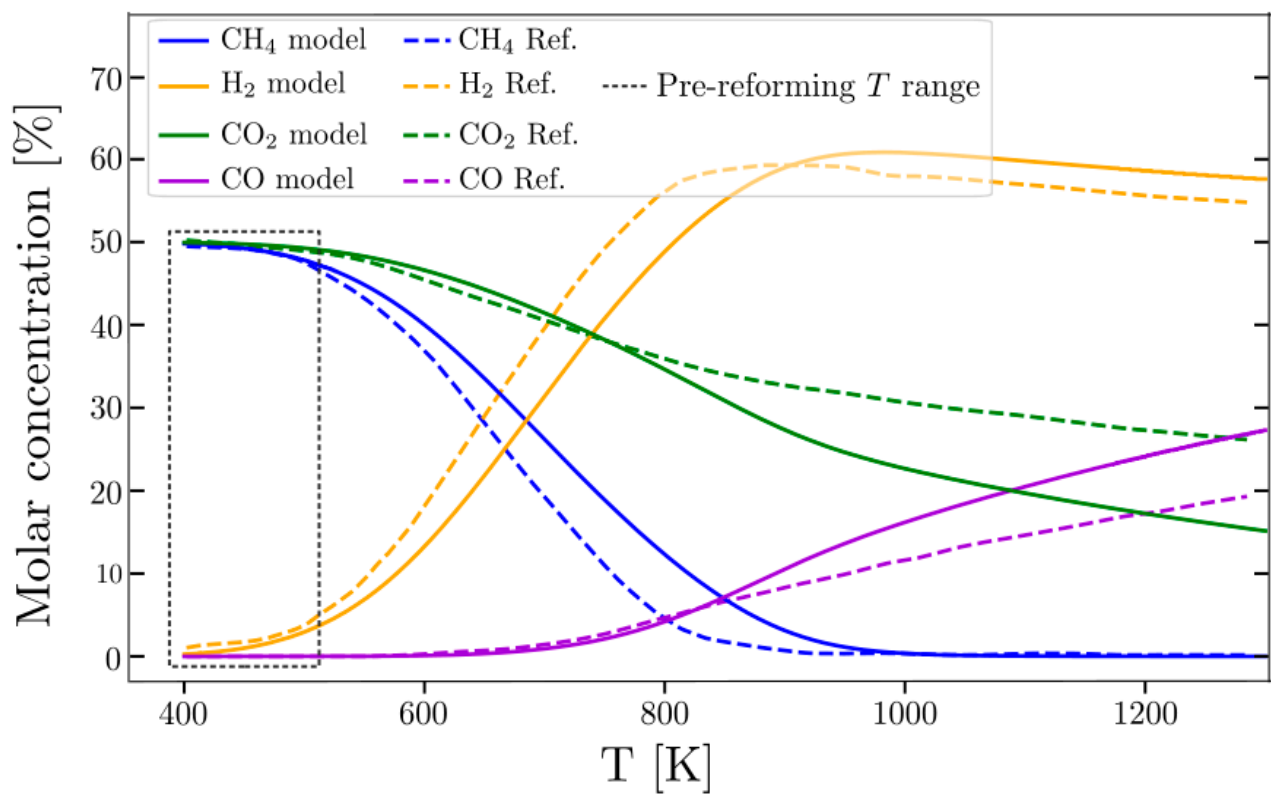
Figure 2. Acetic acid reforming: comparison between the results of the implemented model (solid) and the reported results from [39].
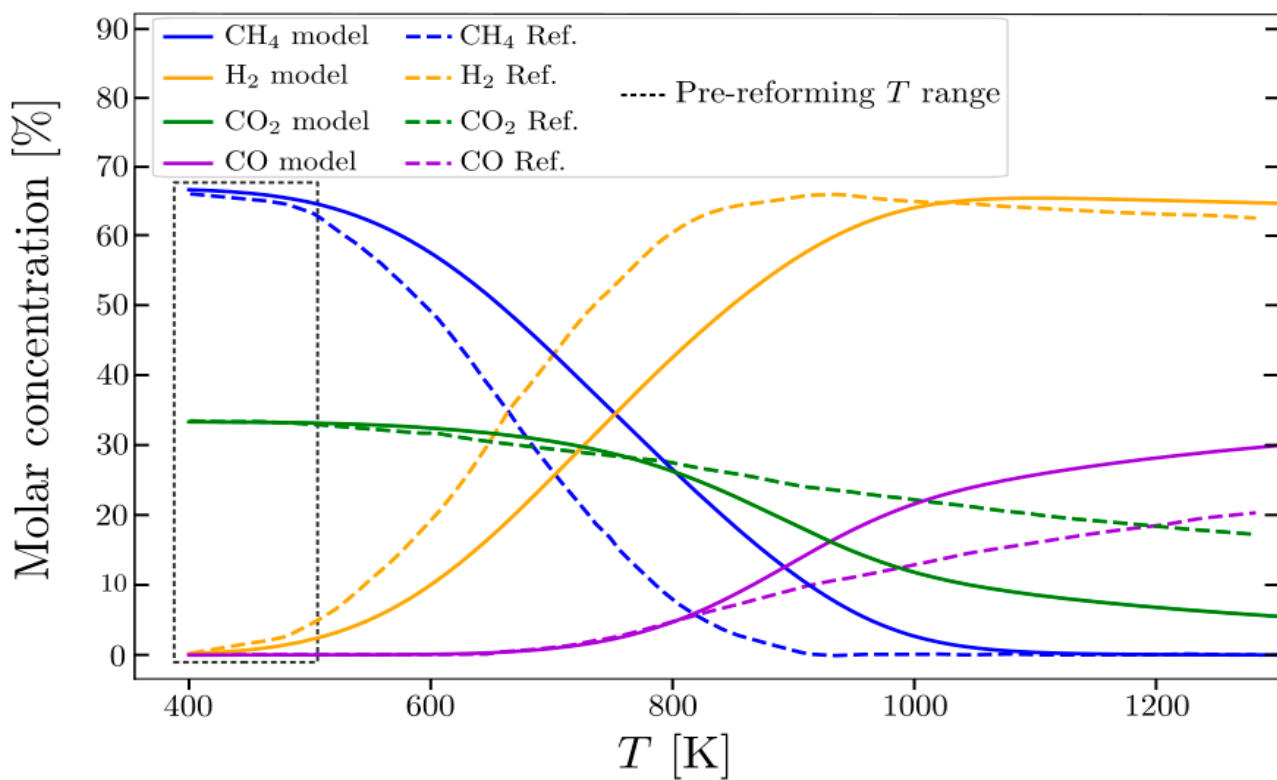
Figure 3. Ethylene glycol reforming: comparison between the results of the implemented model (solid) and the results reported in [39].
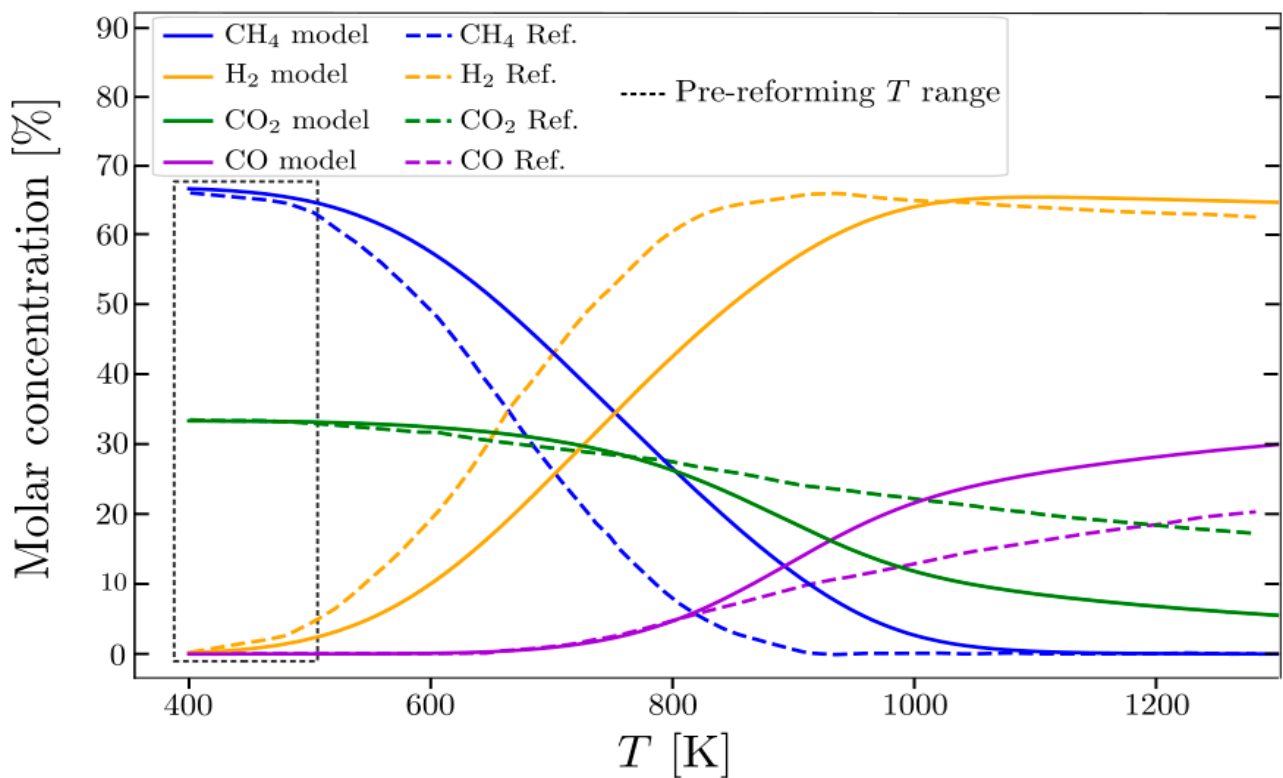
Figure 4. Acetone reforming: comparison between the results of the implemented model (solid) and the results reported in [39].

3.2. Evaluation of the KPIs

The KPIs of the process plant are evaluated for the three different scenarios described in the methodology section. Most of them remain fixed since they are characteristics of the plant itself and do not depend on its operating conditions; they are reported in Table 4.

Table 4. KPIs of the plant independent from the scenarios analyzed.

Performance Parameters		
$m_{H_2,mass}$	[kg/year]	340
$Y_{H_2,mass}$	[%]	5.37%
η	[%]	18.91%
TEC_{mass}	$\left[\dfrac{kWh}{kg_{H_2}}\right]$	315.17
TEC_{vol}	$\left[\dfrac{kWh}{Nm^3 \cdot H_2}\right]$	28.12
EEC_{mass}	$\left[\dfrac{kWh_{ee}}{kg_{H_2}}\right]$	192.35
EEC_{vol}	$\left[\dfrac{kWh_{ee}}{Nm^3 \cdot H_2}\right]$	17.16

The efficiency of the conversion process in terms of energy consumption leads to an electrical specific energy consumption of 17.16 kWh/Nm³$_{H2}$, which is significantly higher than the value that can be achieved by an electrolyzer, characterized by a value of approximately 3–4 kWh/Nm³$_{H2}$ [40,41]. This is driven by the need to have several energy-intensive processes in order to obtain pure hydrogen from residual biomasses. Moreover, the plant produces not only hydrogen but also a crude oil fraction, which can be used for

energy purposes after further upgrading to obtain drop-in fuels. On the other hand, the results achieved in hydrogen yields are remarkable (5.37%) compared to those of other similar conversion systems. For example, a maximum of 4.01% of mass hydrogen yield is obtained by the gasification system proposed in [4], with a much lower concentration of hydrogen purity, approximately 25% vol. Regarding the anaerobic digestion system, as reported in the review of M. Aziz [42], the hydrogen mass yield is always below 3%, significantly lower than the results of this article. This proves that only anaerobic digestion of the feedstock, which is the most suitable treatment for such wet residual biomasses, does not allow the exploitation of all the hydrogen potential, and the combination with a thermochemical treatment allows for good synergies. Indeed, the 55.5% of the total hydrogen production in the proposed plant design is due to the subsequent treatment of pyrolysis by-products, which allows for an increased hydrogen yield compared to the single AD [4], see Figure 5a. This synergy is also observed in other works that combine anaerobic digestion and pyrolysis. In fact, the mass yield of the system that combines anaerobic digestion of corn stover with alkaline pyrolysis reaches a hydrogen mass yield of about 25.9 mmoL/g, or about 5.2% [kg/kg] [43], comparable with the proposed approach. Our approach shows improvement when compared with the work proposed in [44], where a 3% hydrogen yield is reported for a two-stage reactor (pyrolysis and steam reforming) that processes a similar biomass (wheat straw).
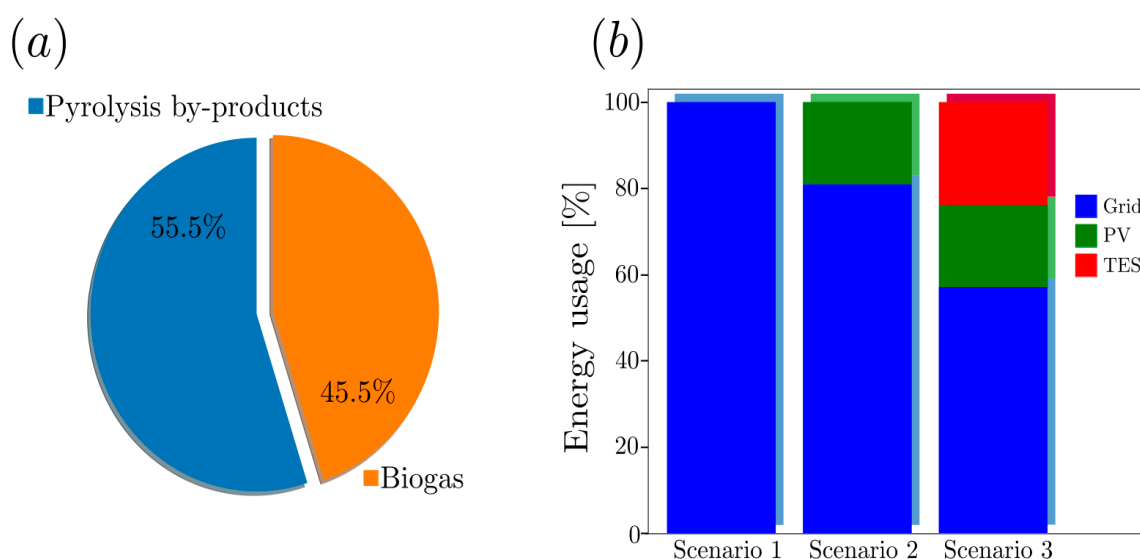
Figure 5. (**a**) Breakdown of the hydrogen contribution by source process; (**b**) Fraction of energy supply by source.

Regarding the KPIs that are more variable among the different scenarios, the values are reported in Table 5, where the key role of the TES is evident. In fact, all values increase dramatically with the introduction of the TES into the system. The emission value is decreased to about 75% of the reference scenario for the case with PV only and drops further to 43% of the reference case in the configuration with PV and TES. As a matter of fact, the self-consumption of Scenario 2 is increased significantly (from 19% to almost 43%), confirming the positive effect of the TES in maximizing the non-programmable RES exploitation in the case studied.

The energy fractions from the different sources are shown in Figure 5b. It is evident that for all the scenarios, the energy from the grid has a major contribution that is reduced to a minimum of 60% with both PV and TES implemented. The PV system powers the plant for about 18% of the overall energy demand, while the TES contributes an even more significant percentage (up to 22%).

Table 5. KPIs of the plant-dependent from the scenarios analyzed.

Performance Parameters				
		Scenario 0	Scenario 1	Scenario 2
$m_{CO_2,tot}$	$[\text{kg/year}]$	10,592	8536	5210
$e_{CO_2,mass}$	$\left[\text{kg}_{CO_2} \middle/ \text{kg}_{H_2} \right]$	31.2	25.1	15.3
$e_{CO_2,Vol}$	$\left[\text{kg}_{CO_2} \middle/ \text{Nm}^3 \cdot \text{H}_2 \right]$	2.78	2.24	1.37
SC	$[\%]$	0	19%	42.8%

4. Conclusions

In this work, an integrated thermochemical plant from residual biomass for the poly-generation of energy carriers, with particular focus on hydrogen, has been evaluated by a preliminary energy and power demand analysis. The effect of the energy supply system is evaluated in terms of energy conversion efficiency, carbon dioxide emissions, and hydrogen production.

The main findings of this work can be summarized according to the following points:

- TES is a key component to achieving a larger self-consumption path for the plant and reducing the carbon footprint of the hydrogen production, reaching a 42.8% self-consumption (SC) value;
- The proposed plant can achieve a specific electrical energy consumption of 17.16 $\left[\text{kWh} \middle/ \text{Nm}^3 \cdot \text{H}_2 \right]$, which is higher if compared to current electrolyzer technologies but can be obtained by valorizing residual low-energy biomasses.
- There is a good synergy in the plant process, reaching a hydrogen yield of 5.37%, demonstrated also by the balance between the hydrogen recovery potential from biogas and pyrolysis products (respectively 44.5% and 55.5%).

Author Contributions: Conceptualization, V.M., L.B. and S.C.; methodology, L.B. and E.D.M.; software, G.D.; validation, G.D.; formal analysis, G.D. and E.D.M.; investigation, G.D. and E.D.M.; resources, V.M. and S.C.; data curation, E.D.M.; writing—original draft preparation, E.D.M., G.D. and L.B.; writing—reviewing and editing, V.M., L.B., M.B. and S.C.; supervision, L.B. and V.M.; visualization, M.B. All authors have read and agreed to the published version of the manuscript.

Appendix A

In this section, a description of the plant subsystems is given.

Appendix A.1. Anaerobic Digestion

AD works in a temperature range of 35 ± 2 °C and a pH of 7 (mesophilic conditions) [6]. The production of biogas at the digester outlet is evaluated using the specific methane production ($CH_{4,Prod,S.}$) obtained from [6]. The dimensions of the digester are such that the pyrolysis reactor can be fed with a digestate flow of 1 kg/h (a dimension imposed by the lab-scale pyrolysis reactor used to validate the model) [29]. The heat demand is assumed to be equal to the heat losses through the digester walls plus the energy needed for substrate

movement. The daily methane production ($Vol_{CH_4, \, dayly}$) accounted for in $\left[\sqrt{\frac{Nl_{CH_4}}{day}} \right]$ is calculated as reported in Equation (A1):

$$Vol_{CH_4, dayly} = CH_{4Prod,S} \cdot OLR \cdot V_{digester}, \tag{A1}$$

where $CH_{4Prod,S}$ represents the specific methane production, OLR is the organic loading rate of the biomass feed, and $V_{digester}$ is the digester volume.

Biogas composition is imposed according to [45] and is equal to 65% methane and 35% carbon dioxide.

Appendix A.2. Pyrolysis

A shaftless screw reactor, studied and built at the laboratory of the "Tor Vergata" University of Rome [29]. The detailed 0/1-D model of the pyrolizer was also developed in [28] and used in this work. This model accurately describes the behavior and performance of a fast pyrolysis process in terms of mass fractions of the three main products of the process (biochar, bio-oil, and syngas), given geometrical parameters and biomass specifications. The model considers both mass and thermal energy balance, and as far as the kinetic part of the reactions is concerned, the DAEM theory (Distributed Activation Energy Model) has been used to calculate the continuous distributed activation energy function f(E). The kinetic framework represents: the activation of virgin biomass; the primary reactions from activated biomass to tar, char, and gas; secondary reactions from tar to gas; and moisture evaporation. The chemical kinetics of the process is described by Arrhenius' first-order irreversible equations, as described in Equation (A2).

$$K_j = A_j \cdot e^{-\left(\frac{E_j}{R \cdot T} \right)}, \tag{A2}$$

where the j represents the j-th chemical group, K is the reaction rate constant, A is the frequency factor, E is the activation energy, R is the universal gas constant, and T is the absolute temperature.

In the model, the heat supplied to the system through the thermal resistor was assumed to occur at a constant wall temperature. In addition, bio-oil condensation is considered for waste heat recovery [46], with a value of 2256 kJ/kg.

Appendix A.3. Electrical Steam Reforming

All products obtained from biomass via anaerobic digestion and pyrolysis were converted into hydrogen through an electrical reformer. This technology gives the opportunity to produce H2 integrated with a renewable source of energy, such as a photovoltaic system. In this way, a hydrogen flow is produced with a much higher conversion rate of biomass, as the reformer is only supplied with electricity [47]. The pre-reformer is a catalytic reactor usually located before the reformer to break down the heavy hydrocarbon chain contained in the feed so that it is easier to reform. In addition to providing a simpler feed to the re-former, the pre-reformer prevents the formation of coke in the primary reactor and the deposition of carbon on the catalytic bed, improving efficiency. The pre-reformer has relatively mild operating conditions in terms of temperature, in the range between 300 °C and 400 °C. Chemical equilibrium is assumed, as often reported in the scientific literature [39,48]. The equilibrium is reached whenever Gibbs free energy is at its minimum. The total Gibbs free energy is calculated as reported in A3.

$$G_{tot} = \sum n_i \cdot \Delta G_{f,i}^0 + \sum n_i \cdot R \cdot T \cdot ln \left(\frac{n_i}{\sum n_i} \right), \tag{A3}$$

where n_i represents the number of moles of the species, "*i*", $G^0_{f,i}$ is the standard Gibbs free energy formation of the species, "*i*", *R* is the universal gas constant, and *T* is the absolute temperature.

The Gibbs free energy is minimized by the Matlab tool "fmincon" using constraining relations:

- Constancy of the number of atoms in each element;
- The number of moles in each species cannot be negative.

Bio-oil is made up of several compounds; only a few have been considered, which according to [39] include acetic acid, ethylene glycol, and acetone.

The model was tested at a temperature of 400 K to 1300 K with a steam-to-carbon ratio of six (S/C = 6) to compare with the results found in the literature [39]. The model was utilized in the system to represent equilibrium conditions depending on the temperature reached by the electrified reformer.

Appendix A.4. Water-Gas-Shift Membrane

Once the products obtained from thermochemical processes leave the reforming section, a mixture of gases rich in hydrogen is obtained. Although in the syngas the concentrations of CO and CO_2 are still high, the mixture must undergo a final upgrading process. Water Gas Shift (WGS) reactors [49] or membranes can be considered for small-scale plants [50].

The TA Pd-based membrane reactor has been considered an interesting technological alternative to increase the conversion of CO and the recovery of H_2 as a result of the continuous removal of hydrogen while the reaction occurs [51], which favors a further shift of the WGS toward the products. Two key parameters for the performance of the membrane reactor in question are the CO conversion (Equation (A4)) and the H_2 recovery (Equation (A5)) as follows:

$$CO_{convertion} = \frac{\dot{n}_{CO,feed} - \dot{n}_{CO,ret}}{\dot{n}_{CO,feed}} , \tag{A4}$$

$$H_{2recovery} = \frac{\dot{n}_{H_2,per}}{\dot{n}_{H_2,feed} + \dot{n}_{CO,feed}} , \tag{A5}$$

where $n_{i,feed}$ represents the flow of the gas component "*i*" in the feed, $n_{i,ret}$ represents the flow of the gas component "*i*" retentate by the membrane reactor, and $n_{i,per}$ represents the flow of the gas component "*i*" permeate through the membrane reactor.

Appendix A.5. Compressor

The specific work of the compression was calculated from the polytropic equation, assuming a polytropic efficiency of 0.8 [52]. The specific work of the compressor is calculated accordingly with Equation (A6):

$$W_{Comp} = \frac{n}{n-1} R \cdot T \left[\left(\frac{p_{max}}{p_{min}} \right)^{\frac{n-1}{n}} - 1 \right] , \tag{A6}$$

where *n* is the polytropic index, *R* is the universal gas constant, and *T* is the absolute temperature, p_{min} and p_{max} are the inlet and outlet pressures of the compressor.

Appendix A.6. Photovoltaic

For the photovoltaic system, a model has been defined based on weather data collected by the Tor Vergata University weather station, which provides radiation and temperature data throughout the year. The model returns the values of current and voltage produced

by the plant based on weather conditions, the panel model in question, and the size of the system itself, considering Maximum Power Point Tracking conditions.

Appendix A.7. Thermal Energy Storage System

The thermal storage system under consideration exploits the capacity of silica sand to retain heat. The heat is supplied to the storage system by the photovoltaic system through electrical resistors when the photovoltaic system is unable to support the whole system's requirements, especially in winter, or whenever a surplus of energy is produced, such as in the summer [53].

References

1. Intergovernmental Panel on Climate Change. *Climate Change 2022: Mitigation of Climate Change—Summary for Policymakers*; Intergovernmental Panel on Climate Change: Geneva, Switzerland, 2022.
2. Intergovernmental Panel on Climate Change. *Climate Change 2022: Impacts, Adaptation and Vulnerability—Summary for Policymakers*; Intergovernmental Panel on Climate Change: Geneva, Switzerland, 2022.
3. Butera, G.; Jensen, S.H.; Gadsbøll, R.; Ahrenfeldt, J.; Clausen, L.R. Flexible biomass conversion to methanol integrating solid oxide cells and TwoStage gasifier. *Fuel* **2020**, *271*, 117654. [CrossRef]
4. Prestipino, M.; Piccolo, A.; Polito, M.F.; Galvagno, A. Combined Bio-Hydrogen, Heat, and Power Production Based on Residual Biomass Gasification: Energy, Exergy, and Renewability Assessment of an Alternative Process Configuration. *Energies* **2022**, *15*, 5524. [CrossRef]
5. Bach, Q.-V.; Nguyen, D.D.; Lee, C.-J. Effect of Torrefaction on Steam Gasification of Biomass in Dual Fluidized Bed Reactor—A Process Simulation Study. *BioEnergy Res.* **2019**, *12*, 1042–1051. [CrossRef]
6. Tayibi, S.; Monlau, F.; Marias, F.; Thevenin, N.; Jimenez, R.; Oukarroum, A.; Alboulkas, A.; Zeroual, Y.; Barakat, A. Industrial symbiosis of anaerobic digestion and pyrolysis: Performances and agricultural interest of coupling biochar and liquid digestate. *Sci. Total Environ.* **2021**, *793*, 148461. [CrossRef] [PubMed]
7. Kevin, A.; Glen, P. The trouble with negative emissions. *Science* **2016**, *354*, 182–183.
8. Burns, W.; Nicholson, S. Bioenergy and carbon capture with storage (BECCS): The prospects and challenges of an emerging climate policy response. *J. Environ. Stud. Sci.* **2017**, *7*, 527–534. [CrossRef]
9. Almena, A.; Thornley, P.; Chong, K.; Röder, M. Carbon dioxide removal potential from decentralised bioenergy with carbon capture and storage (BECCS) and the relevance of operational choices. *Biomass Bioenergy* **2022**, *159*, 106406. [CrossRef]
10. European Commission. The European Green Deal. 2019. Available online: https://eur-lex.europa.eu/resource.html?uri=cellar:b828d165-1c22-11ea-8c1f-01aa75ed71a1.0002.02/DOC_1&format=PDF (accessed on 11 December 2019).
11. Ringkjøb, H.-K.; Haugan, P.M.; Solbrekke, I.M. A review of modelling tools for energy and electricity systems with large shares of variable renewables. *Renew. Sustain. Energy Rev.* **2018**, *96*, 440–459. [CrossRef]
12. Chen, X.; Mcelroy, M.B.; Wu, Q.; Shu, Y.; Xue, Y. Transition towards higher penetration of renewables: An overview of interlinked technical, environmental and socio-economic challenges. *J. Mod. Power Syst. Clean Energy* **2019**, *7*, 1–8. [CrossRef]
13. Arraño-Vargas, F.; Shen, Z.; Jiang, S.; Fletcher, J.; Konstantinou, G. Challenges and Mitigation Measures in Power Systems with High Share of Renewables—The Australian Experience. *Energies* **2022**, *15*, 429. [CrossRef]
14. Guerra, O.J.; Zhang, J.; Eichman, J.; Denholm, P.; Kurtz, J.; Hodge, B.-M. The value of seasonal energy storage technologies for the integration of wind and solar power. *Energy Environ. Sci.* **2020**, *13*, 1909–1922. [CrossRef]
15. Gabrielli, P.; Poluzzi, A.; Kramer, G.J.; Spiers, C.; Mazzotti, M.; Gazzani, M. Seasonal energy storage for zero-emissions multi-energy systems via underground hydrogen storage. *Renew. Sustain. Energy Rev.* **2020**, *121*, 109629. [CrossRef]
16. European Commission. *A Hydrogen Strategy for a Climate-Neutral Europe*; European Commission: Brussels, Belgium, 2020.
17. Ministry of Economy, Trade and Industry (METI). *Ministerial Council on Renewable Energy Hydrogen and Related Issues—Japan Government*; Basic Hydrogen Strategy; Ministry of Economy, Trade and Industry (METI): Tokyo, Japan, 2017; pp. 1–37.
18. Trieb, F.; Moser, M.; Kern, J. Liquid Solar Fuel—Liquid hydrocarbons from solar energy and biomass. *Energy* **2018**, *153*, 1–11. [CrossRef]
19. Poluzzi, A.; Guandalini, G.; D'Amore, F.; Romano, M.C. The Potential of Power and Biomass-to-X Systems in the Decarbonization Challenge: A Critical Review. *Curr. Sustain. Energy Rep.* **2021**, *8*, 242–252. [CrossRef]
20. Henriksen, U.; Ahrenfeldt, J.; Jensen, T.K.; Gøbel, B.; Bentzen, J.D.; Hindsgaul, C.; Sørensen, L.H. The design, construction and operation of a 75kW two-stage gasifier. *Energy* **2006**, *31*, 1542–1553. [CrossRef]
21. Gadsbøll, R.; Clausen, L.; Thomsen, T.P.; Ahrenfeldt, J.; Henriksen, U.B. Flexible TwoStage biomass gasifier designs for polygeneration operation. *Energy* **2019**, *166*, 939–950. [CrossRef]
22. Butera, G.; Jensen, S.H.; Ahrenfeldt, J.; Clausen, L.R. Techno-economic analysis of methanol production units coupling solid oxide cells and thermochemical biomass conversion via the TwoStage gasifier. *Fuel Process. Technol.* **2021**, *215*, 106718. [CrossRef]

23. Bartolucci, L.; Bocci, E.; Cordiner, S.; De Maina, E.; Lombardi, F.; Marcantonio, V.; Mele, P.; Mulone, V.; Sorino, D. Biomass Polygeneration System for the Thermal Conversion of Softwood Waste into Hydrogen and Drop-In Biofuels. *Energies* **2023**, *16*, 1286. [CrossRef]

24. Pecchi, M.; Baratieri, M. Coupling anaerobic digestion with gasification, pyrolysis or hydrothermal carbonization: A review. *Renew. Sustain. Energy Rev.* **2019**, *105*, 462–475. [CrossRef]

25. Kan, X.; Yao, Z.; Zhang, J.; Tong, Y.W.; Yang, W.; Dai, Y.; Wang, C.-H. Energy performance of an integrated bio-and-thermal hybrid system for lignocellulosic biomass waste treatment. *Bioresour. Technol.* **2017**, *228*, 77–88. [CrossRef]

26. Ramachandran, S.; Yao, Z.; You, S.; Massier, T.; Stimming, U.; Wang, C.-H. Life cycle assessment of a sewage sludge and woody biomass co-gasification system. *Energy* **2017**, *137*, 369–376. [CrossRef]

27. Li, Y.; Zhang, R.; He, Y.; Zhang, C.; Liu, X.; Chen, C.; Liu, G. Anaerobic co-digestion of chicken manure and corn stover in batch and continuously stirred tank reactor (CSTR). *Bioresour. Technol.* **2014**, *156*, 342–347. [CrossRef] [PubMed]

28. Luz, F.C.; Cordiner, S.; Manni, A.; Mulone, V.; Rocco, V. Pyrolysis in screw reactors: A 1-D numerical tool. *Energy Procedia* **2017**, *126*, 683–689. [CrossRef]

29. Luz, F.C.; Cordiner, S.; Manni, A.; Mulone, V.; Rocco, V. Biomass fast pyrolysis in screw reactors: Prediction of spent coffee grounds bio-oil production through a monodimensional model. *Energy Convers. Manag.* **2018**, *168*, 98–106. [CrossRef]

30. Bartolucci, L.; Cordiner, S.; Mulone, V.; Pasquale, S.; Sbarra, A. Design and management strategies for low emission building-scale Multi Energy Systems. *Energy* **2022**, *239*, 122160. [CrossRef]

31. Yu, S.; Park, J.; Kim, M.; Ryu, C.; Park, J. Characterization of biochar and byproducts from slow pyrolysis of hinoki cypress. *Bioresour. Technol. Rep.* **2019**, *6*, 217–222. [CrossRef]

32. Kechagiopoulos, P.N.; Voutetakis, S.S.; Lemonidou, A.A.; Vasalos, I.A. Hydrogen Production via Steam Reforming of the Aqueous Phase of Bio-Oil in a Fixed Bed Reactor. *Energy Fuels* **2006**, *20*, 2155–2163. [CrossRef]

33. European Union. Directives Directive (EU) 2018/2001 of the European Parliament and of the Council of 11 December 2018 on the Promotion of the Use of Energy from Renewable Sources (Recast) (Text with EEA Relevance). *Off. J. Eur. Union* **2018**, *L328*, 82–208.

34. Kratzeisen, M.; Starcevic, N.; Martinov, M.; Maurer, C.; Müller, J. Applicability of biogas digestate as solid fuel. *Fuel* **2010**, *89*, 2544–2548. [CrossRef]

35. Available online: https://www.eea.europa.eu/data-and-maps/daviz/co2-emission-intensity-12#tab-googlechartid_chart_11 (accessed on 26 October 2022).

36. Peng, J.; Lu, L.; Yang, H. Review on life cycle assessment of energy payback and greenhouse gas emission of solar photovoltaic systems. *Renew. Sustain. Energy Rev.* **2013**, *19*, 255–274. [CrossRef]

37. Hsu, C.-W. Constructing an evaluation model for hydrogen application pathways. *Int. J. Hydrogen Energy* **2013**, *38*, 15836–15842. [CrossRef]

38. Bridgwater, A.V.; Peacocke, G.V.C. Fast Pyrolysis Processes for Biomass. Available online: www.elsevier.com/locate/rser (accessed on 22 March 2000).

39. Vagia, E.C.; Lemonidou, A.A. Thermodynamic analysis of hydrogen production via autothermal steam reforming of selected components of aqueous bio-oil fraction. *Int. J. Hydrogen Energy* **2008**, *33*, 2489–2500. [CrossRef]

40. Available online: https://ahdb.org.uk/knowledge-library/hydrogen-electrolysis (accessed on 26 January 2022).

41. Koponen, J.; Kosonen, A.; Huoman, K.; Ahola, J.; Ahonen, T.; Ruuskanen, V. Specific energy consumption of PEM water electrolysers in atmospheric and pressurised conditions. In Proceedings of the 2016 18th European Conference on Power Electronics and Applications (EPE'16 ECCE Europe), Karlsruhe, Germany, 5–9 September 2016.

42. Aziz, M.; Darmawan, A.; Juangsa, F.B. Hydrogen production from biomasses and wastes: A technological review. *Int. J. Hydrogen Energy* **2021**, *46*, 33756–33781. [CrossRef]

43. Ting, Z.J.; Raheem, A.; Dastyar, W.; Yang, H.; Dong, W.; Yuan, H.; Li, X.; Wang, W.; Zhang, R.; Zhao, M. Alkaline pyrolysis of anaerobic digestion residue with selective hydrogen production. *Int. J. Hydrogen Energy* **2020**, *45*, 20933–20943. [CrossRef]

44. Lopez, G.; Santamaria, L.; Lemonidou, A.; Zhang, S.; Wu, C.; Sipra, A.T.; Gao, N. Hydrogen generation from biomass by pyrolysis. *Nat. Rev. Methods Prim.* **2022**, *2*, 20. [CrossRef]

45. Tippayawong, N.; Thanompongchart, P. Biogas quality upgrade by simultaneous removal of CO_2 and H_2S in a packed column reactor. *Energy* **2010**, *35*, 4531–4535. [CrossRef]

46. Long, T.; Li, M.; Chen, Y.; Zhu, X. Study on Evaporation Characteristics of Bio-oil and its Compound Models. *Bioresources* **2014**, *9*, 4242–4252. [CrossRef]

47. Wismann, S.T.; Engbæk, J.S.; Vendelbo, S.B.; Eriksen, W.L.; Frandsen, C.; Mortensen, P.M.; Chorkendorff, I. Electrified methane reforming: Elucidating transient phenomena. *Chem. Eng. J.* **2021**, *425*, 131509. [CrossRef]

48. Oladokun, O.; Ahmad, A.; Abdullah, T.A.T.; Nyakuma, B.B.; Kamaroddin, M.F.A.; Nor, S.H.M. Biohydrogen production from Imperata cylindrica bio-oil using non-stoichiometric and thermodynamic model. *Int. J. Hydrogen Energy* **2017**, *42*, 9011–9023. [CrossRef]

49. LeValley, T.L.; Richard, A.R.; Fan, M. The progress in water gas shift and steam reforming hydrogen production technologies—A review. *Int. J. Hydrogen Energy* **2014**, *39*, 16983–17000. [CrossRef]

50. Chen, W.-H.; Chen, C.-Y. Water gas shift reaction for hydrogen production and carbon dioxide capture: A review. *Appl. Energy* **2020**, *258*, 114078. [CrossRef]

51.　Catalano, J.; Guazzone, F.; Mardilovich, I.; Ma, Y.H.; Kazantzis, N. Hydrogen production in a large scale water gas shift pd based membrane reactor. In Proceedings of the Separations Division—Core Programming Topic at the 2011 AIChE Annual Meeting, Minneapolis, MN, USA, 16–21 October 2011; Volume 2, pp. 1258–1259.

52.　Riedl, S.M. Development of a Hydrogen Refueling Station Design Tool. *Int. J. Hydrogen Energy* **2020**, *45*, 1–9. [CrossRef]

53.　Campbell, J. Solidification Structure. In *Complete Casting Handbook*, 2nd ed.; Elsevier: Amsterdam, The Netherlands, 2015. [CrossRef]